

# Descriptor and scaling relations for ion mobility in battery electrodes and solid electrolytes

Mohsen Sotoudeh<sup>1,\*</sup> and Axel Groß<sup>1,2,†</sup>

<sup>1</sup>*Institute of Theoretical Chemistry, Ulm University,*

*Albert-Einstein-Allee 11, 89081 Ulm, Germany*

<sup>2</sup>*Helmholtz Institute Ulm (HIU) for Electrochemical Energy Storage,*

*Helmholtzstraße 11, 89069 Ulm, Germany*

## Abstract

Based on first-principles electronic structure calculations, we have derived an efficient physical descriptor for the ion mobility in battery electrodes and solid electrolytes which is a critical performance parameter in electrochemical energy storage and conversion. This descriptor is entirely composed of observables that are easily accessible: ionic radii, oxidation states and the difference in the Pauling electronegativities of the involved species. Within a particular class of materials, the activation barriers for migration are connected to this migration parameter through linear scaling relations both as far as the variation of the cation chemistry of the charge carriers and the anion chemistry of the host lattice are concerned. The validity of these scaling relations indicates that a purely ionic view of ion mobility in solids falls short of capturing all factors influencing this mobility. The identification of these scaling relations has the potential to significantly accelerate the discovery of materials with desired mobility properties.

Keywords: ion mobility, descriptor, scaling relations, mono- and multivalent charge carriers, density functional theory

---

\* mohsen.sotoudeh@uni-ulm.de

† axel.gross@uni-ulm.de

## 22 I. INTRODUCTION

23 Electrochemical energy storage devices play a central role in our attempts towards de-  
24 carbonization through the storage of volatile renewable energy and the emission-free usage  
25 of vehicles and mobile devices. Significant progress has been made in this respect due to  
26 the development of advanced Li-ion battery technologies<sup>1,2</sup>. In addition, recently so-called  
27 post Li-ion technologies have drawn a lot of attention in order to address, among others,  
28 sustainability issues associated with the materials typically used in Li-ion batteries<sup>3,4</sup>. In  
29 post-Li ion batteries, other charge carriers such as monovalent Na and K cations<sup>5,6</sup> or diva-  
30 lent Mg and Ca cations<sup>7-11</sup> are used. These post-Li-ion batteries can compete with existing  
31 Li-ion batteries as far as efficiency and safety are concerned<sup>12,13</sup> or even exhibit a better  
32 performance, in particular with respect to safety aspects<sup>14-18</sup>. In addition, batteries based  
33 on divalent cations such as Mg<sup>2+</sup> can achieve higher volumetric energy densities compared  
34 to monovalent-based batteries<sup>12,13</sup>. Furthermore, as liquid electrolytes are prone to corro-  
35 sion processes and often represent fire hazards because of their flammability, all solid-state  
36 batteries with higher safety and better electrochemical stability<sup>19</sup> based on materials such  
37 as inorganic oxides<sup>20,21</sup>, hydrides<sup>22-24</sup>, and chalcogenides<sup>25,26</sup> have been intensively studied  
38 for all possible charge carriers.

39 A critical parameter that significantly influences the performance of batteries is the ion  
40 mobility both in the electrolyte and in the electrodes<sup>27-29</sup>. Unfortunately, the efficiency of  
41 particularly batteries based on multivalent ions such as Mg<sup>2+</sup> is hampered by a low ion  
42 mobility<sup>30-32</sup> due to the strong interaction of the multivalent ions with the host structures.  
43 Hence the identification and development of materials with improved ion mobility are es-  
44 sential for more efficient electrochemical energy storage devices.

45 A very useful concept in order to accelerate materials discovery is based on so-called de-  
46 scriptors<sup>33,34</sup>. They represent fundamental materials properties or combinations thereof that  
47 are correlated with a desired or undesired functionality of the material. This concept has  
48 been very successfully used in heterogeneous catalysis<sup>35</sup>, in particular in connection with  
49 so-called scaling relations<sup>36</sup>, but also already in battery research<sup>18</sup>. The identification of  
50 descriptors can significantly speed up the search for new materials with desired functional  
51 properties because once they are identified only the particular descriptors need to be opti-  
52 mized in a first step. Thus promising candidate materials can be proposed whose properties

53 can then be scrutinized in detail.

54 In fact, also with respect to ion mobility in solids a number of possible descriptors have  
55 been proposed, based on the lattice volume and ionic size<sup>26,27</sup>, the choice of the anion sub-  
56 lattice<sup>27,37</sup>, the lattice dynamics<sup>27,38</sup>, or the preferred crystal insertion site<sup>28</sup>. However, many  
57 of the identified descriptors are restricted to some particular crystal structure. Furthermore,  
58 some are based on materials properties that are not easily accessible. Hence it is fair to say  
59 that so far no convenient descriptor has been established that is able to predict ion mobility  
60 across a set of different structures.

61 Based on the results of first-principles density functional theory (DFT) calculations and  
62 physico-chemical reasoning, here we propose such a convenient descriptor for the ion mobil-  
63 ity, the so-called migration parameter or number, that is based on the product of Pauling's  
64 electronegativity, ionic radii and oxidation states of the involved compounds, all properties  
65 that are easily accessible for any material. This particular descriptor, whose choice is also  
66 supported by a statistical analysis of our first-principles results, goes beyond current propos-  
67 als by considering also deviations from a purely ionic interaction between the migrating ion  
68 and the host lattice. According to our calculations, the activation barrier for migration is  
69 connected to this migration number via linear scaling relations that are different for different  
70 classes of materials. This allows to predict the activation barriers both for the variation of  
71 the cation chemistry of the migrating ion as well as for the variation of the anion chemistry  
72 of the host lattice. Thus this descriptor will most probably significantly accelerate the dis-  
73 covery of materials with favorable mobility properties. As this migration number is based  
74 on basic physico-chemical quantities, it also enables a deeper fundamental understanding of  
75 the principles underlying ion mobility.

## 76 II. RESULTS AND DISCUSSION

77 From a microscopic viewpoint, migration or diffusion in solid crystalline materials occurs  
78 by atomic hops in a lattice. Such jump processes are typically thermally activated, and the  
79 corresponding tracer diffusion coefficient is given by

$$D^{\text{tr}} = D_0^{\text{tr}} \exp\left(-\frac{E_a}{k_{\text{B}}T}\right). \quad (1)$$

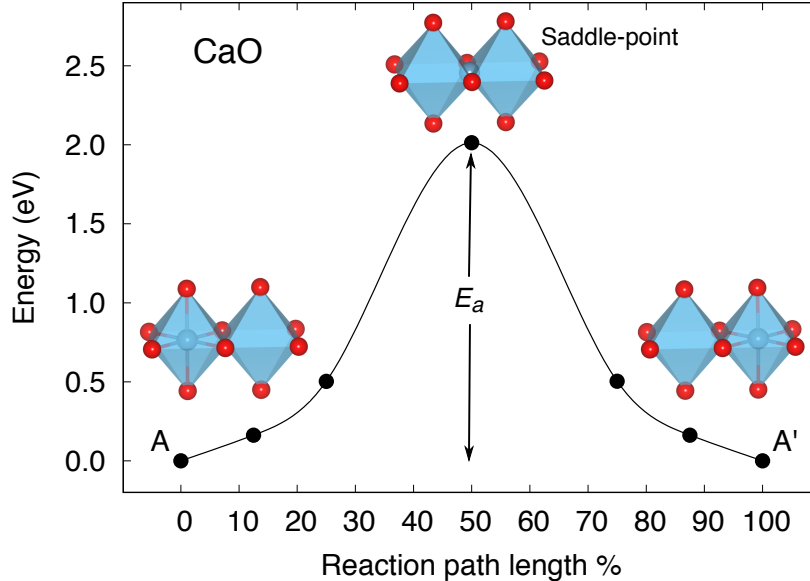


FIG. 1. Illustration of a cation interstitial migration mechanism, using Ca diffusion in CaO as an example. A diffusion event corresponds to the migration of the Ca cation from the energetically most favorable octahedral site A to the nearest equivalent site A' through the transition state which corresponds to a saddle-point in the multi-dimensional potential energy surface and which can be derived by first-principles electronic structure calculations. The activation energy or diffusion barrier is denoted by  $E_a$  which corresponds to the energy difference between the saddle-point and the initial configuration.

80 Here  $D_0^{\text{tr}}$  is the pre-exponential factor,  $k_B$  the Boltzmann constant, and  $T$  the absolute  
 81 temperature.  $E_a$  is the activation barrier corresponding to the energy barrier along the  
 82 minimum energy path connecting two equivalent intercalation sites, as illustrated in Fig. 1.  
 83 Such an minimum energy path can be determined by automatic search routines<sup>39</sup>. In the  
 84 present work, we have used the nudged elastic band method (NEB)<sup>40</sup> in the DFT calcu-  
 85 lations to derive the activation barrier  $E_a$ . The electronic structure calculations were per-  
 86 formed using the Vienna *Ab-initio* Simulation Package (VASP)<sup>41</sup> employing the Projector  
 87 Augmented Wave (PAW)<sup>42</sup> method with the exchange-correlation effects being described  
 88 with the Perdew-Burke-Ernzerhof (PBE) functional<sup>43</sup>. Further details are provided in the  
 89 supporting information.

90 Motivated by the goal to identify the fundamental factors determining ion mobility in  
 91 solids, in a previous study<sup>26</sup> we had derived the activation barriers for diffusion of a number

of ions of varying size and charge in the same host lattice, a chalcogenide spinel. We obtained the expected results, namely that the size and the charge of the diffusing ion matter. However, the ionic radius of the charge carrier alone could not explain the observed trends, but rather the distance between the ion in the tetrahedral site and the nearest chalcogenide atom. In order to further elucidate the mobility-determining factors, we decided to look at structurally simpler compounds, namely binary  $A_nX_m$  materials with A being the migrating ion. In total, we looked at 35 different compounds with Li, Mg, and Ca as the migrating ion A.

For these binary materials, we again found that size and charge of the propagating ions matter, but not in a very systematic way, as already observed by others<sup>27</sup>. However, we could recently show that the stability of ions in chalcogenide spinels can only be understood if deviations from a purely ionic interaction are taken into account<sup>44</sup>. It is essential to realize that the considered binary materials span the whole range of interaction characteristics between metallic and ionic bonding. Such bonding characteristics can in fact be classified in so-called Van Arkel-Ketelaar triangles<sup>45</sup> in which compounds are placed according to the mean electronegativity  $\chi_{mean}$  ( $x$ -axis) and the electronegativity difference  $\Delta\chi$  ( $y$ -axis) of the constituting elements.

Fig. 2a shows the Van Arkel-Ketelaar triangle including the Mg binary compounds considered in this study. A large difference in electronegativity indicates ionic bonding characteristics (shown in yellow), as present in MgO and MgF<sub>2</sub>. CsF (not shown) would lie at the apex of the triangle. At the bottom of the triangle corresponding to small electronegativity difference, an increasing mean electronegativity is associated with more directional bonding. Hence the lower left corner contains metallic systems whereas the lower right corner gathers covalent systems.

The  $Mg_nX_m$  binaries considered in this study all fall along a line between metallic and ionic bonding. The green area in Fig. 2a corresponds to a region of bonding characteristic intermediate between ionic and metallic. In detail, MgF<sub>2</sub> has the highest electronegativity difference  $\Delta\chi$  indicating a strong ionic bond. This is also true for MgO, whereas Mg<sub>2</sub>Si is associated with the lowest value  $\Delta\chi$  demonstrating metallic bonding. The rest of Mg-halides, Mg-chalcogenides, Mg-pnictides, and Mg-tetrels are located between strong ionic and metallic bonding. They are divided into three groups. MgCl<sub>2</sub>, MgBr<sub>2</sub>, and Mg<sub>3</sub>N<sub>2</sub> are characterized by a large electronegativity difference of about 1.7 demonstrating a predomi-

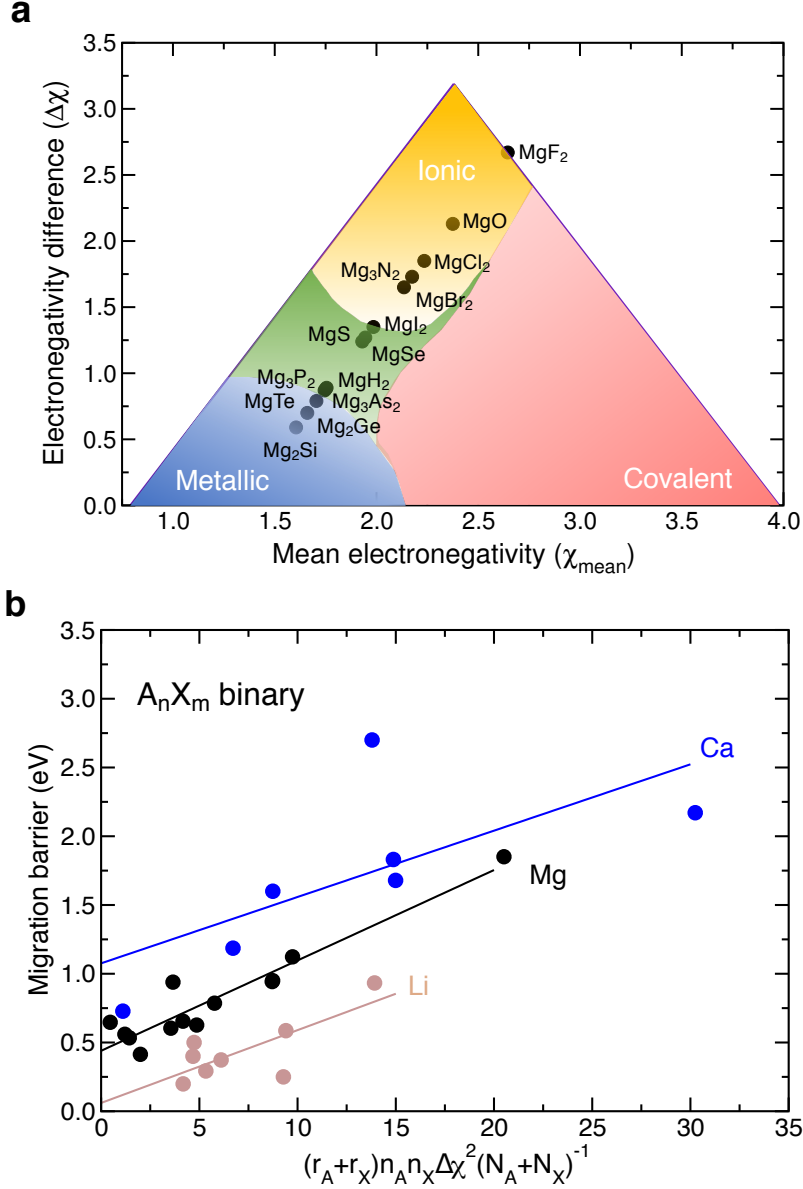


FIG. 2.  $A_nX_m$  binaries considered in this study. (a) Van Arkel-Ketelaar triangle with the considered  $Mg_nX_m$  binaries plotted as a function of the mean electronegativity and the difference in the electronegativity of the two components. (b) Calculated activation energies for the migration of  $A = \text{Li}, \text{Mg}, \text{and Ca}$  in  $A_nX_m$  binaries as a function of the migration number  $N_{\text{migr}}^{\text{AX}}$  for various elements  $X$  according to Eq. (2). The solid lines correspond to linear regressions of these results.

124 nately ionic bonding (light yellow region).  $\text{MgI}_2$ ,  $\text{MgS}$ , and  $\text{MgSe}$  have  $\Delta\chi \approx 1.3$ , the other  
 125  $\text{Mg}$  binaries have electronegativity differences below 1.

126 The fact that also non-ionic components of the interaction contribute to the bonding

127 in nominally ionic crystals<sup>44</sup> suggests that also the interaction characteristics within the  
 128 considered compounds represented by the electronegativity difference  $\Delta\chi^2$  influences the  
 129 ion mobility. Together with the well-known dependence of the diffusion barriers on the ionic  
 130 radii ( $r_i$ ) and oxidation states ( $n_i$ ) of the involved compounds, this observation motivated  
 131 us to define the *migration* parameter or number  $N_{\text{migr}}$

$$N_{\text{migr}}^{\text{AX}} = (r_{\text{A}} + r_{\text{X}})n_{\text{A}}n_{\text{X}}\Delta\chi_{\text{AX}}^2/(N_{\text{A}} + N_{\text{X}}) \quad (2)$$

132 as the product of these three quantities where the ionic radii are given in Å,  $n_{\text{A}}$  and  $n_{\text{X}}$   
 133 are the absolute values of the formal integer oxidation states or numbers. In addition, also  
 134 the number of atoms of the corresponding species in the unit cell of the crystal  $N_{\text{A}}$  and  $N_{\text{X}}$   
 135 enters. In Fig. 2b, we plot the dependence of the migration barriers as a function of the  
 136 migration parameter for the three migrating ions Li, Mg and Ca in the low vacancy limit. In  
 137 spite of some outliers, overall the migration barriers nicely follow separate scaling relations  
 138 for each migrating ion

$$E_a^{\text{A}}(\text{X}) = E_0^{\text{A}} + C^{\text{A}}(r_{\text{A}} + r_{\text{X}})n_{\text{A}}n_{\text{X}}\Delta\chi_{\text{AX}}^2/(N_{\text{A}} + N_{\text{X}}) = E_0^{\text{A}} + C^{\text{A}}N_{\text{migr}}^{\text{AX}}. \quad (3)$$

139 These universal scaling relations strongly suggest that the same factors govern the ion mo-  
 140 bility in all considered binary compounds. The outliers indicate that other critical contribu-  
 141 tions to the activation energies such as Coulomb interactions beyond those represented by  
 142 the oxidation states, quantum mechanical overlap effects and polarization<sup>27</sup> can play a role.

143 In order to verify that we identified the crucial parameters governing ion mobility in  
 144 these binary materials, we applied a statistical compressed-sensing approach using the sure-  
 145 independence screening and sparsifying operator SISO<sup>46</sup>, as described in detail in the sup-  
 146 porting information, to search for possible descriptors. We used the following input param-  
 147 eters or so-called primary features: number of atoms in the unit-cell ( $N_{\text{atom}}$ ) and the atomic  
 148 masses of the two elements in the binary compound ( $m_{\text{A}}, m_{\text{X}}$ ), their formal oxidation  
 149 numbers ( $n_{\text{A}}, n_{\text{X}}$ ) and ionic radii ( $r_{\text{A}}, r_{\text{X}}$ ), the Pauling electronegativity ( $\chi_{\text{A}}, \chi_{\text{X}}$ ) of both  
 150 elements, the A-X bond distances  $d_{\text{A-X}}$ , and the unit cell volume  $V$ . This approach allows  
 151 to vary the dimensionality  $\Omega$  of the descriptor space, and the descriptor is expressed as a  
 152 linear combination of so-called features that are non-linear functions of the input parameter  
 153 or primary features. For  $\Omega = 1$ , we obtained the descriptor

$$d = (((n_{\text{X}}/n_{\text{A}}) - \cos(n_{\text{X}}))/((\chi_{\text{X}})^6 \cdot \sin(m_{\text{X}}))) , \quad (4)$$

154 whereas for  $\Omega = 2$  we found a two-dimensional descriptor consisting of the two features  $d_1$   
 155 and  $d_2$ :

$$d_1 = (n_X)^2 \times (r_{\text{Mg}} + r_X) , \quad (5)$$

$$d_2 = (\chi_X)^3 / (N_{\text{atom}}) . \quad (6)$$

156 Indeed these findings confirm that the oxidation states reflecting the charge of the atoms,  
 157 the ion radii and the electronegativity differences are the determining factors for the migra-  
 158 tion barriers. Interestingly, the unit cell volume  $V$  which has been shown to substantially  
 159 influence the ionic mobility in some structural families<sup>26,27</sup> does not show up in these sta-  
 160 tistically derived descriptors. However, note that the functional dependencies found by the  
 161 SISO operators do not allow for a straightforward interpretation of the physico-chemical  
 162 factors underlying the migration process.

163 Therefore we decided to look for a verification whether the observed scaling relations as a  
 164 function of the migration parameter (Eq. (2)) are also valid for other material types. As this  
 165 study was originally motivated by the results for migration barriers of  $A^{n+}$  in  $\text{AB}_2\text{X}_4$  spinel  
 166 structures, we reconsidered our previous results. For these structures, the NEB method was  
 167 again applied in the low vacancy limit. In Fig. 3, we have plotted the migration barriers  
 168  $E_a$  (in eV) as a function of the migration parameter Eq. (2) for  $\text{ASc}_2\text{S}_4$  and  $\text{MgSc}_2\text{X}_4$  spinels  
 169 (panel a) and  $\text{ACr}_2\text{S}_4$  and  $\text{MgCr}_2\text{X}_4$  spinels (panel b), respectively. Note that the factor  
 170  $1/(N_A + N_X)$  has been omitted in the definition of the  $x$ -axis as this factor is constant  
 171 for all considered materials. Again, as in Fig. 2, we find a linear scaling of the migration  
 172 barriers upon variation of the anions  $X^{n-}$  (blue symbols). Interestingly enough, we also find  
 173 additional scaling relations upon variation of the cations  $\text{Li}^+$ ,  $\text{Na}^+$ ,  $\text{K}^+$ ,  $\text{Mg}^{2+}$ ,  $\text{Ca}^{2+}$ , and  
 174  $\text{Sr}^{2+}$  (black symbols) (note that the  $\text{MgSc}_2\text{S}_4$  and  $\text{MgCr}_2\text{S}_4$  spinels, respectively, are part of  
 175 both corresponding subsets). These results demonstrate that the scaling relations Eq. (3)  
 176 are independently valid for the variation of both the cation chemistry of the migrating ions  
 177  $A^{n+}$  as well as for the variation of the anion chemistry of the host lattice ions  $X^{n-}$ .

178 As Fig. 3 illustrates, upon variation of the host lattice cations  $B^{n+}$  present in the sulfide  
 179 spinels  $\text{AB}_2\text{X}_4$ , which are typically transition metal cations, the slope of the linear scaling  
 180 relations represented by the parameter  $C^A$  in Eq. 2 changes. We have determined the height  
 181 of the migration barriers for the six additional transition metals  $B = \text{Ti}, \text{V}, \text{Mn}, \text{Fe}, \text{Co}$  and  
 182  $\text{Ni}$  as a function of the migration number upon variation of the migrating cations  $A^{n+}$  and

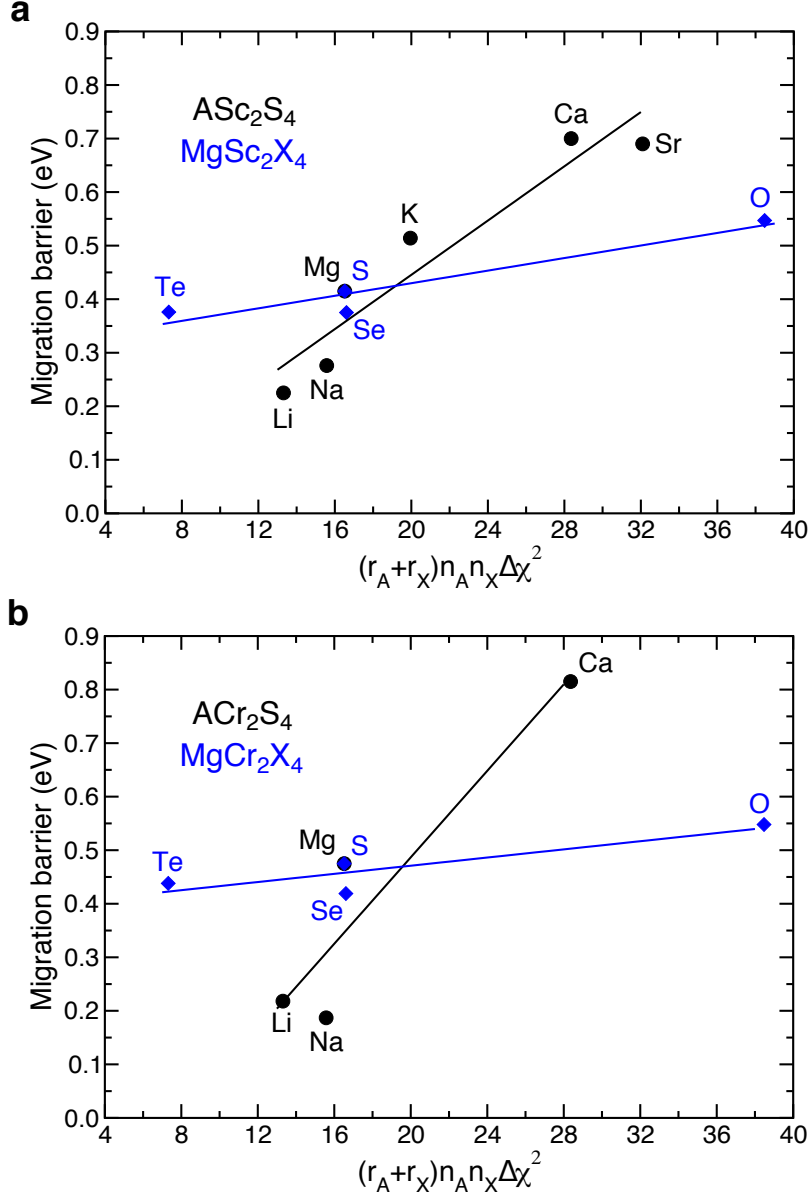


FIG. 3. Panel a: migration barriers (in eV) in  $A\text{Sc}_2\text{X}_4$  as a function of the migration parameter  $(r_A + r_X)n_A n_X \Delta \chi_{AX}^2$  (Eq. (2)) for  $A\text{Sc}_2\text{X}_4$  (black symbols) and  $\text{MgSc}_2\text{X}_4$  spinels (blue symbols) for various mono- and multivalent cations  $A^{n+}$  and anions  $X^{n-}$ . Panel b: the same as in panel a, but with Sc replaced by Cr.

183 collected the results in Fig. 4. We again find that the migration barriers follow linear scaling  
 184 relations, but with different slopes. It is interesting to note that the difference  $\Delta E_a^A(B)$   
 185 between the lowest and the highest migration barrier upon variation of the eight considered  
 186 transition metals B increase with the size and the charge of the migrating cations  $A^{n+}$ , as

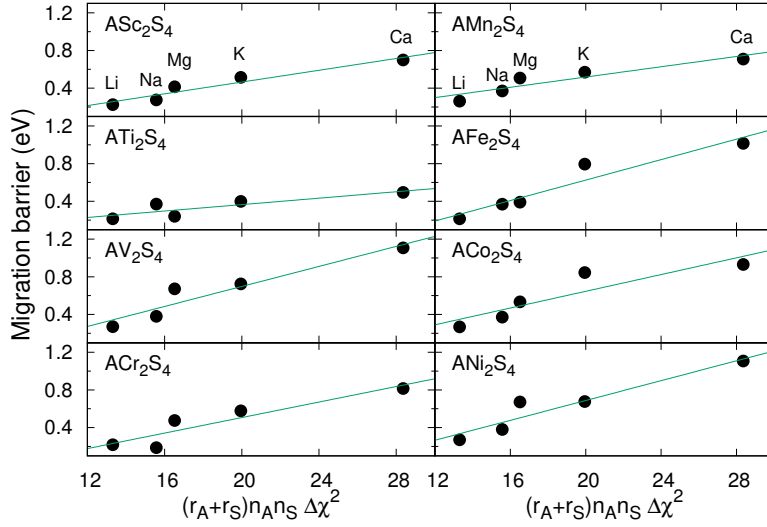


FIG. 4. Migration barriers (in eV) in  $AB_2S_4$  spinels as a function of the migration number  $N_{\text{migr}}^{\text{AS}}$  for eight different transition metal cations  $B = \text{Sc, Ti, V, Cr, Mn, Fe, Co}$  and  $\text{Ni}$  upon variation of migrating cations  $A = \text{Mg, Na, K, Mg, and Ca}$ .

187 illustrated in Tab. I. Apparently for increasing charge and size of the host lattice cations  $B$ ,  
 188 the specific nature of the interaction between the cations  $A$  and  $B$  becomes more prominent,  
 189 as far as the migration barriers for  $A$  are concerned.

190 We have tried to derive some more trends in the height of the migration barrier as a  
 191 function of the squared electronegativity difference between transition metal  $B$  and anion  $X$ ,  
 192  $\Delta\chi_{\text{BX}}^2$ , and the ionic radius  $r_B$  of the transition metal  $B$  (see supporting information, Fig. S1).  
 193 Indeed, we find pronounced minima in  $E_a$  as a function of these variables, but we did not  
 194 manage to identify any linear scaling relations upon the variation of the cation  $B$ . However,  
 195 based on the identification of these pronounced minima and the corresponding matching

TABLE I. Difference  $\Delta E_a^A(B)$  in eV between the lowest and the highest migration barrier for the charge carriers  $A = \text{Li, Na, K, Mg}$  and  $\text{Na}$  in  $AB_2X_4$  spinels upon variation of the eight considered transition metals  $B$  shown in Fig. 4.

Migrating ion	$\text{Li}^+$	$\text{Na}^+$	$\text{K}^+$	$\text{Mg}^{2+}$	$\text{Ca}^{2+}$
$\Delta E_a^A(B)$ (eV)	0.08	0.19	0.42	0.44	0.61

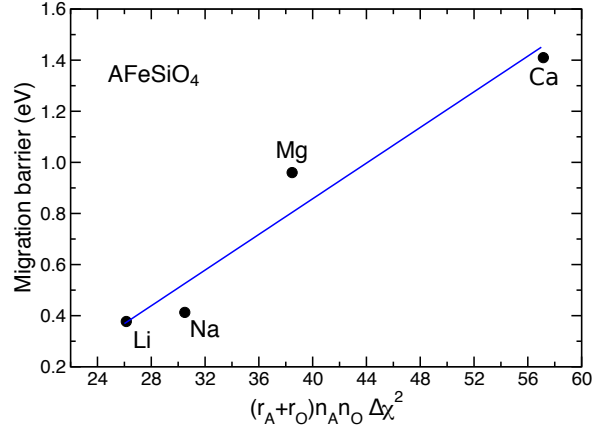


FIG. 5. Migration barriers (in eV) in the olivine  $\text{AFeSiO}_4$  as a function of the migration parameter  $(r_A + r_X)n_A n_X \Delta\chi_{AX}^2$  (Eq. (2)) for varying charge carriers A.

196 properties of Zr, we identified  $\text{MgZr}_2\text{S}_4$  as a promising ion conductor with a high ion mobility,  
 197 and indeed we found that  $\text{MgZr}_2\text{S}_4$  has a rather low Mg migration barrier of only 0.3 eV.

198 We have applied the concept to yet another class of materials that are widely used as  
 199 battery materials, namely olivines<sup>47</sup>. Figure 5 shows the migration barriers in the olivine  
 200  $\text{AFeSiO}_4$  as a function of the migration parameter  $(r_A + r_O)n_A n_X \Delta\chi_{AO}^2$  (Eq. (2)) for varying  
 201 charge carriers A. Again a convincing linear scaling relation has been obtained.

202 The fact that the migration parameter  $N_{\text{migr}}^{\text{AX}}$  captures the essence of the migration barrier  
 203 height upon variation of the migrating cation A and the anion X of the host lattice calls for a  
 204 critical assessment of this parameter. There are some obvious factors influencing the height  
 205 of the migration barrier. For larger ions it will be harder to migrate through a given lattice,  
 206 therefore it is no surprise that the ion radius  $r_A$  enters the migration barrier. However, when  
 207 also varying the size of the anion of the host lattice, it becomes apparent that it is both  
 208 the size of the cation and of the anion represented by  $r_A + r_X$  that is the critical length  
 209 parameter, as already stressed in a previous study<sup>26</sup>. Furthermore, note that in many cases  
 210 the dependence of the mobility on the ionic radius is not monotonic<sup>27</sup>, so any descriptor  
 211 of the ion mobility taking into account the ionic radius needs to reflect this non-monotonic  
 212 behavior.

213 It is also well-known that the charge of the migrating ion matters with respect to the ion  
 214 mobility. The higher the charge of an ion, the stronger its interaction with the environment  
 215 and thus the higher the migration barriers. This same argumentation of course also applies

216 to the charge of the ions constituting the host lattice as the ionic interaction scales with  
217 the product of the charges of interacting ions. These charges enter the migration parameter  
218 through the product of the oxidation numbers  $n_A n_X$ .

219 However, it is important to realize that in the migration of “ions” in a host lattice it is  
220 not *a priori* clear that the “ions” keep their ionic charge. Any crystal containing migrating  
221 ions has to be overall charge neutral because macroscopically charged matter is unstable.  
222 Hence any charge on the migrating ions has to be compensated by the host lattice. Of  
223 course, the assumption that strong ions remain charged in a host lattice makes a lot of sense  
224 and is the basis of the concept of formal oxidation numbers. Still, formal atomic charges in  
225 a material are no good observables because it can not be uniquely defined which electrons  
226 belong to the migration ion and which to the host lattice. This is also the reason why there  
227 is a broad variety of different charge partition schemes used in quantum chemical codes in  
228 order to derive atomic charge numbers which can give quite different quantitative results.  
229 And furthermore, there are hardly any chemical systems in which the interaction is either  
230 purely ionic or purely covalent or purely metallic. Therefore it is not surprising that trends  
231 in the ion mobility can not be fully understood on the basis of formal oxidation states alone.

232 This deviation from the purely ionic interaction can be characterized by the difference in  
233 the electronegativity  $\Delta\chi^2$  of the interacting compounds which is also the basis for the Van  
234 Arkel-Ketelaar triangle. In this context it should be noted that the Pauling electronegativity  
235 in the form revised by Allred<sup>48</sup> that has been used here is based on a quite accurate, semi-  
236 empirical formula for dissociation energies, namely

$$(\chi_A - \chi_B)^2 = E_d(\text{AB}) - \frac{E_d(\text{AA}) + E_d(\text{BB})}{2}. \quad (7)$$

237 This illustrates that the square of the difference in the electronegativities takes the deviation  
238 from a purely ionic interaction in a compound crystal into account. It is in fact true that  
239 the stronger polarizability of “soft” anions has already been used to explain the higher ion  
240 mobility in chalcogenides containing sulfur and selenide compared to oxides<sup>11</sup> with their  
241 softness reflected in the lower electronegativity of sulfur and selenide<sup>49,50</sup>. Still this notion  
242 had not been transferred into any descriptor concept before.

243 The fact that the migration parameter including  $\Delta\chi^2$  yields such a good descriptor for  
244 the height of the migration barriers reconfirms that a purely ionic consideration of ion  
245 mobility in crystals does not capture all factors determining this mobility. It also means

246 that this deviation from ionicity is the reason for the observed non-monotonic behavior of  
247 the migration barriers as a function of the ionic radii which is correctly taken into account  
248 by including the factor  $\Delta\chi^2$  in the migration parameter. It is also important to stress the  
249 fact that the parameters entering the migration number are basically independent of the  
250 particular structure of the considered host lattice, as they correspond to general atomic and  
251 ionic properties of the particular elements. The same parameters enter the scaling relations  
252 for binaries, spinels and olivines, confirming the general fundamental nature of the scaling  
253 relations.

254 Note that the linear scaling relations as a function of the migration parameter established  
255 in our work do not allow the quantitative prediction of the height of migration barriers in  
256 any particular system without any initially measured or calculated data. Thus they do not  
257 correspond to a parameterization of the barrier height as a function of input parameter across  
258 all families of possible structures. However, these scaling relations allow to make qualitative  
259 predictions of the height of migration barriers, and once some migration barriers are known in  
260 these structures, then even semi-quantitative predictions based on easily accessible materials  
261 parameters can be made. This will be very beneficial for the identification of promising  
262 candidate materials with improved mobility properties. Of course, this linear scaling is not  
263 perfect, and we already identified some outliers. However, this descriptor is based on a  
264 strict physico-chemical reasoning, so deviations from the scaling relations should point to  
265 some interesting additional factors also influencing the ion mobility and thus to an enhanced  
266 fundamental understanding of ion mobility.

### 267 **III. CONCLUSIONS AND SUMMARY**

268 In summary, we propose a descriptor called migration parameter for the ion mobility in  
269 crystalline solids that is based on well-accessible materials parameters, namely ion sizes,  
270 oxidation states and the Pauling electronegativity difference between anions and cations in  
271 the compounds. Thus in contrast to previous attempts to derive descriptors for the ion  
272 mobility we also take the deviation from ionic bonding in the compounds into account. For  
273 a broad range of materials classes, we have shown that the height of the migration barrier  
274 follows linear scaling relations as a function of this descriptor upon both the variation of the  
275 cation chemistry of the migrating ion as well as upon variation of the anion chemistry of the

276 host lattice. This demonstrates the strong predictive power of the descriptor which should  
277 accelerate the discovery of materials with improved migration properties in electrochemical  
278 energy storage and conversion.

## 279 **ACKNOWLEDGMENTS**

280 Useful discussions with Jürgen Janek, University of Gießen, and Holger Euchner, Helmholtz-  
281 Institute Ulm, are gratefully acknowledged. This work contributes to the research performed  
282 at CELEST (Center for Electrochemical Energy Storage Ulm-Karlsruhe) and was funded  
283 by the German Research Foundation (DFG) under Project ID 390874152 (POLiS Cluster  
284 of Excellence). Further support by the Dr. Barbara Mez-Starck Foundation and computer  
285 time provided by the state of Baden-Württemberg through bwHPC and the German Re-  
286 search Foundation (DFG) through grant no INST 40/467-1 FUGG (JUSTUS cluster) are  
287 gratefully acknowledged.

## 288 **AUTHOR CONTRIBUTIONS**

289 AG designed and supervised the whole project. MS developed the conceptual framework  
290 of the project, performed all calculations and wrote the first draft of the manuscript. Both  
291 authors revised the manuscript and have approved the submitted version.

---

292 <sup>1</sup> Sinho Choi and Guoxiu Wang, “Advanced lithium-ion batteries for practical applications: Tech-  
293 nology, development, and future perspectives,” *Adv. Mater. Technol.* **3**, 1700376 (2018).

294 <sup>2</sup> Yanjiao Ma, Yuan Ma, Gabriele Giuli, Holger Euchner, Axel Groß, Giovanni Orazio Lepore,  
295 Francesco d’Acapito, Dorin Geiger, Johannes Biskupek, Ute Kaiser, Hanno M. Schütz, Anna  
296 Carlsson, Thomas Diemant, Rolf Jürgen Behm, Matthias Kuenzel, Stefano Passerini, and  
297 Dominic Bresser, “Introducing highly redox-active atomic centers into insertion-type electrodes  
298 for lithium-ion batteries,” *Adv. Energy Mater.* **10**, 2000783 (2020).

299 <sup>3</sup> Giuseppe Antonio Elia, Krystan Marquardt, Katrin Hoepfner, Sebastien Fantini, Rongying Lin,  
300 Etienne Knipping, Willi Peters, Jean-Francois Drillet, Stefano Passerini, and Robert Hahn, “An  
301 overview and future perspectives of aluminum batteries,” *Adv. Mater.* **28**, 7564–7579 (2016).

- 302 <sup>4</sup> M. Anji Reddy, M. Helen, Axel Groß, Maximilian Fichtner, and Holger Euchner, “Insight into  
303 sodium insertion and the storage mechanism in hard carbon,” *ACS Energy Lett.* **3**, 2851–2857  
304 (2018).
- 305 <sup>5</sup> Jang-Yeon Hwang, Seung-Taek Myung, and Yang-Kook Sun, “Sodium-ion batteries: present  
306 and future,” *Chem. Soc. Rev.* **46**, 3529–3614 (2017).
- 307 <sup>6</sup> Naoaki Yabuuchi, Kei Kubota, Mouad Dahbi, and Shinichi Komaba, “Research development  
308 on sodium-ion batteries,” *Chem. Rev.* **114**, 11636–11682 (2014).
- 309 <sup>7</sup> Thomas D. Gregory, Ronald J. Hoffman, and Richard C. Winterton, “Nonaqueous electro-  
310 chemistry of magnesium: Applications to energy storage,” *J. Electrochem. Soc.* **137**, 775–780  
311 (1990).
- 312 <sup>8</sup> D. Aurbach, Z. Lu, A. Schechter, Y. Gofer, H. Gizbar, R. Turgeman, Y. Cohen, M. Moshkovich,  
313 and E. Levi, “Prototype systems for rechargeable magnesium batteries,” *Nature* **407**, 724–727  
314 (2000).
- 315 <sup>9</sup> Christina M. MacLaughlin, “Status and outlook for magnesium battery technologies: A conver-  
316 sation with Stan Whittingham and Sarbajit Banerjee,” *ACS Energy Lett.* **4**, 572–575 (2019).
- 317 <sup>10</sup> Rachel Davidson, Ankit Verma, David Santos, Feng Hao, Cole D. Fincher, Dexin Zhao, Vahid  
318 Attari, Parker Schofield, Jonathan Van Buskirk, Antonio Fraticelli-Cartagena, Theodore E. G.  
319 Alivio, Raymundo Arroyave, Kelvin Xie, Matt Pharr, Partha P. Mukherjee, and Sarbajit  
320 Banerjee, “Mapping mechanisms and growth regimes of magnesium electrodeposition at high  
321 current densities,” *Mater. Horiz.* **7**, 843–854 (2020).
- 322 <sup>11</sup> Fabio Maroni, Saustin Dongmo, Cornelius Gauckler, Mario Marinaro, and Margret Wolfahrt-  
323 Mehrens, “Through the maze of multivalent-ion batteries: A critical review on the status of  
324 the research on cathode materials for Mg<sup>2+</sup> and Ca<sup>2+</sup> ions insertion,” *Batteries & Supercaps*  
325 (2021), <https://doi.org/10.1002/batt.202000330>.
- 326 <sup>12</sup> Nikhilendra Singh, Timothy S. Arthur, Chen Ling, Masaki Matsui, and Fuminori Mizuno, “A  
327 high energy-density tin anode for rechargeable magnesium-ion batteries,” *Chem. Commun.* **49**,  
328 149–151 (2013).
- 329 <sup>13</sup> Zhirong Zhao-Karger, Maria Elisa Gil Bardaji, Olaf Fuhr, and Maximilian Fichtner, “A new  
330 class of non-corrosive, highly efficient electrolytes for rechargeable magnesium batteries,” *J.*  
331 *Mater. Chem. A* **5**, 10815–10820 (2017).

- 332 <sup>14</sup> D. Aurbach, Y. Cohen, and M. Moshkovich, “The study of reversible magnesium deposition  
333 by in situ scanning tunneling microscopy,” *Electrochem. Solid-State Lett.* **4**, A113 (2001).
- 334 <sup>15</sup> M. Matsui, “Study on electrochemically deposited Mg metal,” *J. Power Sources* **196**, 7048 –  
335 7055 (2011).
- 336 <sup>16</sup> Q. S. Zhao and J. L. Wang, “Reversibility of electrochemical magnesium deposition from  
337 tetrahydrofuran solutions containing pyrrolidinyll magnesium halide,” *Electrochim. Acta* **56**,  
338 6530 (2011).
- 339 <sup>17</sup> Markus Jäckle and Axel Groß, “Microscopic properties of lithium, sodium, and magnesium  
340 battery anode materials related to possible dendrite growth,” *J. Chem. Phys.* **141**, 174710  
341 (2014).
- 342 <sup>18</sup> Markus Jäckle, Katharina Helmbrecht, Malte Smits, Daniel Stottmeister, and Axel Groß, “Self-  
343 diffusion barriers: Possible descriptors for dendrite growth in batteries?” *Energy Environ. Sci.*  
344 **11**, 3400–3407 (2018).
- 345 <sup>19</sup> Jürgen Janek and Wolfgang G. Zeier, “A solid future for battery development,” *Nature Energy*  
346 **1**, 16141 (2016).
- 347 <sup>20</sup> Shoichiro Ikeda, Masatoshi Takahashi, Junichi Ishikawa, and Kaname Ito, “Solid electrolytes  
348 with multivalent cation conduction. 1. Conducting species in Mg-Zr-PO<sub>4</sub> system,” *Solid State*  
349 *Ionics* **23**, 125 – 129 (1987).
- 350 <sup>21</sup> Z.A. Halim, S.B.R.S. Adnan, and N.S. Mohamed, “Effect of sintering temperature on the struc-  
351 tural, electrical and electrochemical properties of novel Mg<sub>0.5</sub>Si<sub>2</sub>(PO<sub>4</sub>)<sub>3</sub> ceramic electrolytes,”  
352 *Ceram. Int.* **42**, 4452 – 4461 (2016).
- 353 <sup>22</sup> Rana Mohtadi, Masaki Matsui, Timothy S. Arthur, and Son-Jong Hwang, “Magnesium boro-  
354 hydride: From hydrogen storage to magnesium battery,” *Angew. Chem. Int. Ed.* **51**, 9780–9783  
355 (2012).
- 356 <sup>23</sup> Atsushi Unemoto, Motoaki Matsuo, and Shin-ichi Orimo, “Complex hydrides for electrochem-  
357 ical energy storage,” *Adv. Funct. Mater.* **24**, 2267–2279 (2014).
- 358 <sup>24</sup> Shougo Higashi, Kazutoshi Miwa, Masakazu Aoki, and Kensuke Takechi, “A novel inorganic  
359 solid state ion conductor for rechargeable Mg batteries,” *Chem. Commun.* **50**, 1320–1322 (2014).
- 360 <sup>25</sup> Pieremanuele Canepa, Shou-Hang Bo, Gopalakrishnan Sai Gautam, Baris Key, William D.  
361 Richards, Tan Shi, Yaosen Tian, Yan Wang, Juchuan Li, and Gerbrand Ceder, “High magne-  
362 sium mobility in ternary spinel chalcogenides,” *Nat. Commun.* **8**, 1759 (2017).

- 363 <sup>26</sup> Manuel Dillenz, Mohsen Sotoudeh, Holger Euchner, and Axel Groß, “Screening of charge carrier  
364 migration in the MgSc<sub>2</sub>Se<sub>4</sub> spinel structure,” *Front. Energy Res.* **8**, 260 (2020).
- 365 <sup>27</sup> John Christopher Bachman, Sokseiha Muy, Alexis Grimaud, Hao-Hsun Chang, Nir Pour, Si-  
366 mon F. Lux, Odysseas Paschos, Filippo Maglia, Saskia Lupart, Peter Lamp, Livia Giordano,  
367 and Yang Shao-Horn, “Inorganic solid-state electrolytes for lithium batteries: Mechanisms and  
368 properties governing ion conduction,” *Chem. Rev.* **116**, 140–162 (2016).
- 369 <sup>28</sup> Ziqin Rong, Rahul Malik, Pieremanuele Canepa, Gopalakrishnan Sai Gautam, Miao Liu, Anub-  
370 hav Jain, Kristin Persson, and Gerbrand Ceder, “Materials design rules for multivalent ion  
371 mobility in intercalation structures,” *Chem. Mater.* **27**, 6016–6021 (2015).
- 372 <sup>29</sup> Holger Euchner, Jin Hyun Chang, and Axel Groß, “On stability and kinetics of Li-rich transition  
373 metal oxides and oxyfluorides,” *J. Mater. Chem. A* **8**, 7956–7967 (2020).
- 374 <sup>30</sup> E. Levi, Y. Gofer, and D. Aurbach, “On the way to rechargeable Mg batteries: The challenge  
375 of new cathode materials,” *Chem. Mater.* **22**, 860–868 (2010).
- 376 <sup>31</sup> Matthew M. Huie, David C. Bock, Esther S. Takeuchi, Amy C. Marschilok, and Kenneth J.  
377 Takeuchi, “Cathode materials for magnesium and magnesium-ion based batteries,” *Coord.*  
378 *Chem. Rev.* **287**, 15 – 27 (2015).
- 379 <sup>32</sup> Vivek Verma, Sonal Kumar, William Manalastas Jr., Rohit Satish, and Madhavi Srinivasan,  
380 “Progress in rechargeable aqueous zinc- and aluminum-ion battery electrodes: Challenges and  
381 outlook,” *Adv. Sustainable Syst.* **3**, 1800111 (2019).
- 382 <sup>33</sup> Luca M. Ghiringhelli, Jan Vybiral, Sergey V. Levchenko, Claudia Draxl, and Matthias Scheffler,  
383 “Big Data of materials science: Critical role of the descriptor,” *Phys. Rev. Lett.* **114**, 105503  
384 (2015).
- 385 <sup>34</sup> Olexandr Isayev, Corey Oses, Cormac Toher, Eric Gossett, Stefano Curtarolo, and Alexander  
386 Tropsha, “Universal fragment descriptors for predicting properties of inorganic crystals,” *Nat.*  
387 *Commun.* **8**, 15679 (2017).
- 388 <sup>35</sup> J. K. Nørskov, J. Rossmeisl, A. Logadottir, L. Lindqvist, J. R. Kitchin, T. Bligaard, and  
389 H. Jónsson, “Origin of the overpotential for oxygen reduction at a fuel-cell cathode,” *J. Phys.*  
390 *Chem. B* **108**, 17886–17892 (2004).
- 391 <sup>36</sup> Isabela C. Man, Hai-Yan Su, Federico Calle-Vallejo, Heine A. Hansen, Jose I. Martinez, Nilay G.  
392 Inoglu, John Kitchin, Thomas F. Jaramillo, Jens K. Nørskov, and Jan Rossmeisl, “Universality  
393 in oxygen evolution electrocatalysis on oxide surfaces,” *ChemCatChem* **3**, 1159–1165 (2011).

- 394 <sup>37</sup> Yan Wang, William Davidson Richards, Shyue Ping Ong, Lincoln J. Miara, Jae Chul Kim, Yifei  
395 Mo, and Gerbrand Ceder, “Design principles for solid-state lithium superionic conductors,” *Nat.*  
396 *Mater.* **14**, 1026 (2015).
- 397 <sup>38</sup> Sokseiha Muy, John C. Bachman, Livia Giordano, Hao-Hsun Chang, Douglas L. Abernathy,  
398 Dipanshu Bansal, Olivier Delaire, Satoshi Hori, Ryoji Kanno, Filippo Maglia, Saskia Lupart,  
399 Peter Lamp, and Yang Shao-Horn, “Tuning mobility and stability of lithium ion conductors  
400 based on lattice dynamics,” *Energy Environ. Sci.* **11**, 850–859 (2018).
- 401 <sup>39</sup> Ann-Kathrin Henß, Sung Sakong, Philipp K. Messer, Joachim Wiechers, Rolf Schuster, Don C.  
402 Lamb, Axel Groß, and Joost Wintterlin, “Density fluctuations as door-opener for diffusion on  
403 crowded surfaces,” *Science* **363**, 715–718 (2019).
- 404 <sup>40</sup> Graeme Henkelman and Hannes Jónsson, “Improved tangent estimate in the nudged elastic  
405 band method for finding minimum energy paths and saddle points,” *J. Chem. Phys.* **113**, 9978  
406 (2000).
- 407 <sup>41</sup> G. Kresse and J. Furthmüller, “Efficient iterative schemes for ab initio total-energy calculations  
408 using a plane-wave basis set,” *Phys. Rev. B* **54**, 11169–11186 (1996).
- 409 <sup>42</sup> P. E. Blöchl, “Projector augmented-wave method,” *Phys. Rev. B* **50**, 17953–17979 (1994).
- 410 <sup>43</sup> John P. Perdew, Kieron Burke, and Matthias Ernzerhof, “Generalized gradient approximation  
411 made simple,” *Phys. Rev. Lett.* **77**, 3865–3868 (1996).
- 412 <sup>44</sup> Mohsen Sotoudeh, Manuel Dillenz, and Axel Groß, “Mechanism of magnesium transport in  
413 spinel chalcogenides,” *Nature Materials* (2020), submitted.
- 414 <sup>45</sup> Leland C. Allen, Joseph F. Capitani, Gary A. Kolks, and Gordon D. Sproul, “Van  
415 Arkel—Ketelaar triangles,” *J. Mol. Struct.* **300**, 647–655 (1993).
- 416 <sup>46</sup> Runhai Ouyang, Stefano Curtarolo, Emre Ahmetcik, Matthias Scheffler, and Luca M. Ghir-  
417 inghelli, “SISSO: A compressed-sensing method for identifying the best low-dimensional de-  
418 scriptor in an immensity of offered candidates,” *Phys. Rev. Materials* **2**, 083802 (2018).
- 419 <sup>47</sup> N.G. Hörmann and A. Groß, “Stability, composition and properties of  $\text{Li}_2\text{FeSiO}_4$  surfaces stud-  
420 ied by DFT,” *J. Solid State Electrochem.* **18**, 1401–1413 (2014).
- 421 <sup>48</sup> A.L. Allred, “Electronegativity values from thermochemical data,” *J. Inorg. Nucl. Chem.* **17**,  
422 215 – 221 (1961).
- 423 <sup>49</sup> Miao Liu, Anubhav Jain, Ziqin Rong, Xiaohui Qu, Pieremanuele Canepa, Rahul Malik, Ger-  
424 brand Ceder, and Kristin A. Persson, “Evaluation of sulfur spinel compounds for multivalent

425 battery cathode applications,” *Energy Environ. Sci.* **9**, 3201–3209 (2016).  
426 <sup>50</sup> Minglei Mao, Xiao Ji, Singyuk Hou, Tao Gao, Fei Wang, Long Chen, Xiulin Fan, Ji Chen,  
427 Jianmin Ma, and Chunsheng Wang, “Tuning anionic chemistry to improve kinetics of Mg  
428 intercalation,” *Chem. Mater.* **31**, 3183–3191 (2019).